14th World Congress in Computational Mechanics (WCCM)
ECCOMAS Congress 2020
19 – 24 July 2020, Paris, France
F. Chinesta, R. Abgrall, O. Allix and M. Kaliske (Eds)

ANALYSES ON FRICTION STIR BASED TECHNIQUES TO JOIN LIGHTWEIGHT ALLOYS TO THERMOPLASTIC MATRIX PARTS

F. GAGLIARDI[1], G. SERRATORE[1], R. IBANEZ[2], E. CUETO[3], L. FILICE[1] AND F. CHINESTA[2]

[1]DIMEG - University of Calabria
P. Bucci 45/C, Rende (Cs) 87036
{francesco.gagliardi, giuseppe.serratore, luigino.filice}@unical.it

[2]ESI Group Chair @ PIMM, Arts et Métiers ParisTech
151 Boulevard de l'Hôpital, F-75013 Paris, France.
{ruben.ibanez-pinillo, francisco.CHINESTA}@ensam.eu

[3]Department of Mechanical Engineering – University of Zaragoza
Maria de Luna, Zaragoza, Spain 50018
ecueto@unizar.es

Key words: Mechanical Fastening, Dissimilar materials, Friction Stir Techniques, Machine Learning, Advanced regression, Data-Driven Techniques.

Abstract. Nowadays, the manufacturing research efforts have to be conceived in such a way that the product performance criteria are achieved in a lightweighting design concept. Taking these extensions to their extreme, the material properties and the manufacturing solutions have to be considered together in a revolutionary body concept, which should result in an ideal sight to the use of the most performing material in the right place depending on the product requirements. Polymer matrix composites (PMCs) belong to this new material category. The development of joining techniques available to connect PMCs and lightweight alloys has been considered as a key enabling solution in making innovative and sustainable products. The goal of obtaining high joint efficiency must face two main problems, i.e. to deal with the polymeric matrices to get mechanical, physical and chemical compatibilities and to attain or preserve the integrity of reinforcements across the joints customizing the fiber distribution in the joining area.

The understanding of current and emerging joining technologies, e.g. the friction stir based techniques, with an optimization of the process parameters needs performant numerical tools to be employed, efficiently. In the work herein proposed, a polymeric base plate was joined to an aluminum alloy part simulating the friction lap joint sequences. Numerical tests have been set by a commercial FE code (DEFORM 2D^{TM}) and a DoE, generated using hypercube sampling, was defined to perform a sensitivity analysis of specific investigated variables on some process outputs. A further objective is to create transfer functions involving the input and output quantities of interest. Particularly, the sparse Proper Generalized Decomposition (sPGD) is the implemented numerical algorithm that making use of two ingredients, the separation of

variables together with a collocation procedure, allows achieving a prediction tool usable in improving the process performance.

1 INTRODUCTION

Aluminum alloys and thermoplastic materials are widely used today to achieve lightweight concept design, for example in the automotive industries for reducing vehicle weights. A challenge is the development of joining techniques available to connect these materials through the optimization of innovative and sustainable joints.

This goal is not easy to reach if materials with dissimilar properties, such as PMCs and metals, need to be connected. Specifically, when an Aluminum alloy is joined with a thermoplastic material two issues arise, i.e. to deal with the polymeric matrices to get mechanical, physical and chemical compatibilities and to attain or preserve the integrity of reinforcements across the joints customizing the fiber distribution in the joining area. The understanding of current and emerging joining technologies according to the mechanisms of joint formation is, therefore, a key issue in boosting the manufacturing of composites. Among the mechanical fastening solutions, the friction stir based techniques have been developing in different variants [1,2]. Friction Spot Joining (FSpJ) represents one of the most promising solid-phase joining techniques. FSpJ is an innovative technique patented by Helmholtz-Zentrum Geesthacht in Germany [3] for producing thin-sheet metal-polymer joints. The process is based on the friction spot welding technology used to weld metals and thermoplastics [4].

The spot joints are executed through a non-consumable tool composed of two movable parts, called pin and sleeve, which are mounted coaxially to a clamping ring, with the purpose to ensure contact between the parts to be connected. Both pin and sleeve are characterized by a rotational speed, which allows heating the joined area. The generated heat depends on other two process parameters that are: the plunge depth of the pin inside the metallic sheet and the joining time, whose phases are schematized in Fig. 1.

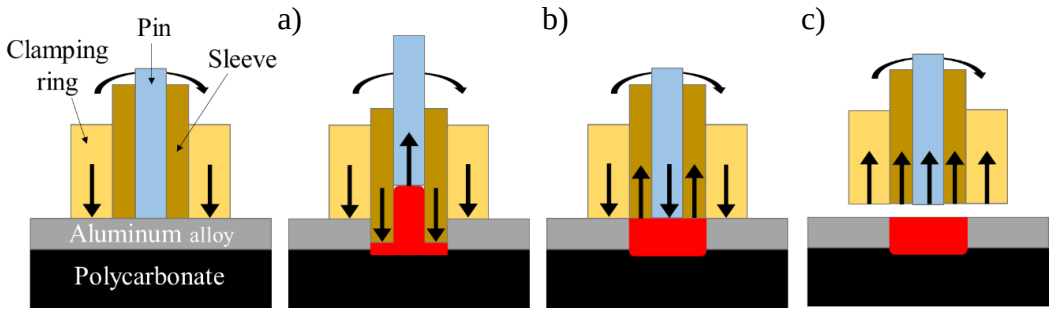

Figure 1: Schematic illustration of the Friction Spot Joining Process. The Sleeve plunging softens the Aluminum alloy (a); spot refilling (b) and joint consolidation (c).

Since this is an innovative and complex joining solution, several researches have been carried out from an experimental and numerical point of view [5,6]. Complex dynamics have to be considered, such as a material stirring, high deformation, heat flow, combination of material with different thermal and material flow properties, etc. The numerical models available in literature adaptable to the FSjP refer to the friction spot welding process for joining

materials [7–11]. The main problem is the mesh distortion owing to the stirring effect of the tool rotation that is computationally expensive to solve and that could result in a premature simulation failure. Therefore, herein, the research has been focalized on setting of a simple but efficient 2D axisymmetric numerical model, which can be used to evaluate specific process outputs, which go to affect the behavior of the resulting joints. Furthermore, a statistical experimental plan was defined to analyze the influence of some identified variables on specific process outputs and an advanced regression technique was employed to predict the process answer at different working conditions.

2 METHODOLOGY

Two aluminium alloys, characterized by different mechanical properties, were joined individually to a polycarbonate plate. This section outlines a description of the adopted methodology. Specifically, the finite element model developed for the FSpJ, the Design of experiment (DoE) planning and the sparse Proper Generalized Decomposition (sPGD) technique are described.

2.1 Model description

The starting point is the development of a performant numerical tool suitable for the analysis and prediction of the FSpJ process, efficiently. To do this, the "Torsion" mode in the geometry section of DEFORM 2D^{TM} was employed in order to reproduce the heat flow caused by the friction interaction, without excessively increasing the computational effort. The main assumption of this model is to neglect the material stirring that could be simulated only with a 3D approach.

The present model is composed of two deformable plates and three rigid body elements representing the tool. The aluminum part was considered with a thickness of 1.5 mm while the polycarbonate 2.17 mm-thick, in accordance with ASTM D3528 for the double lap shear (DLS) joint specimen geometry. The tool dimensions used in this paper are: a diameter of 6 mm for the Pin, a diameter of 9 mm for the sleeve and a diameter of 14.5 mm for the clamping ring [5]. Initially, the number of elements is approximatively around 2500. Fig. 2 shows the adopted 2D axisymmetric finite element model.

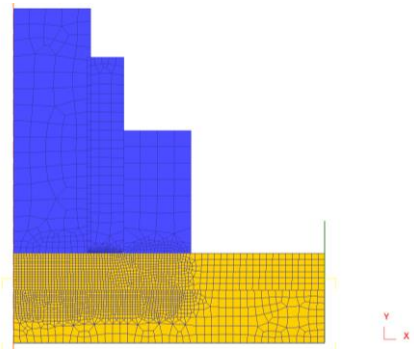

Figure 2: 2D Axisymmetric finite element model for the FSpJ process simulation

A coulomb friction coefficient of 0.5 was set between the aluminum and the polycarbonate

sheet while a shear coefficient of 0.5 was considered among the other surfaces[12]. Finally, a 0.2 [13] N/mm/s/°C heat transfer coefficient was set between the aluminum and the polycarbonate. The constitutive material models of the aluminum alloys, i.e., the AA 1050 and AA 2024 were expressed by Johnson-Cook's model [14], which considers the effects of strain hardening, thermal softening, and strain rate sensitivity, respectively. Table 1 provides the Johnson-Cook parameters for both materials. The thermal and elastic properties were considered as temperature-dependent in all simulations.

Table 1: Johnson-Cook plasticity model constant for AA 1050 [15] and AA 2024 [16]

Material	A [MPa]	B [MPa]	C	n	m	T_{room} [°C]	T_{melt} [°C]
AA 1050	110	150	0.01	0.4	1	20	645
AA 2024	352	440	0.0083	0.42	1	20	640

Regarding the polycarbonate, the constitutive material model was expressed by the DSGZ [17], a viscoplastic phenomenological model developed for glassy or semi-crystalline polymers. This model considers the effect of the strain, strain rate, temperature, softening and hardening. The eight coefficients used are listed in Table 2.

Table 2: Material coefficent for polycarbonate [17]

Material	C_1	C_2	m	a(K)	K (MPa s^m)	$C_3(s^m)$	C_4	α
Polycarbonate	4.02	0.038	415	28.4	0.03	5.8	5.8	6.8

2.2 Performed Numerical simulations according to a planned DoE

This section defines the numerical tests generated with DoE through hypercube sampling to minimize the number of required simulations. As explained in the introduction, many process parameters affect the FSpJ joint efficiency and, at the same time, these parameters interact with the others making difficult to weight each influence on the entire process. Therefore, a DoE based on Latin Hypercube sampling, was employed investigating four process parameters, i.e. rotational speed, plunge depth, joining time and type of aluminum alloy, as reported in Table 3. For the sake of clarity, Fig. 3 shows the phases simulated with the FE model, according to Fig.1a and Fig.1b.

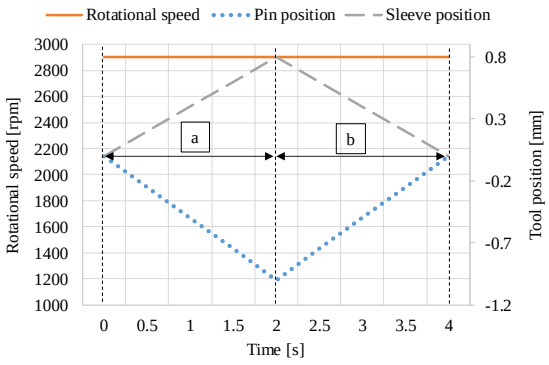

Figure 3: Variation monitoring diagram of the "a" and "b" FSpJ process phases considered in this work.

Table 3: FSpJ process parameters and their respective levels (min, max and step)

Factors	Symbol	Unit	Min	Max	Step
Rotational speed	RS	rpm	1000	3000	100
Plunge depth	PD	mm	0.5	1	0.1
Joining time	JT	s	4	8	0.5
Material	-	-	AA 1050	AA 2024	-

Additionally, the DoE was generated considering a total of 30 simulations, which results in 30 joining conditions as reported in Table 4, where the analyzed ranges can be detected.

Table 4: DoE matrix listing the 30 joining conditions

Joining condition	Factors			
	RS (rpm)	PD (mm)	JT (s)	Material
1	2000	0.7	6	AA 1050
2	2800	0.7	4.5	AA 2024
3	1700	1	6	AA 1050
4	2100	0.6	5	AA 2024
5	1900	1	7.5	AA 1050
6	1400	0.6	8	AA 2024
7	2200	0.8	8	AA 2024
8	1500	0.9	7	AA 1050
9	1100	0.6	6	AA 2024
10	1000	0.5	5	AA 1050
11	2500	0.6	6	AA 1050
12	3000	0.5	7	AA 1050
13	2600	0.6	7.5	AA 2024
14	2600	0.8	6.5	AA 1050
15	1500	1	5.5	AA 2024
16	2400	0.9	5	AA 2024
17	2800	0.6	7	AA 2024
18	1600	0.9	5.5	AA 1050
19	1200	0.7	5	AA 2024
20	2300	0.8	4	AA 1050
21	1500	0.7	4.5	AA 1050
22	1200	0.9	6.5	AA 2024
23	1800	0.7	4.5	AA 1050
24	2700	0.9	5	AA 2024
25	2200	0.7	7.5	AA 1050
26	2400	0.9	7	AA 2024
27	1700	0.8	6.5	AA 1050
28	2900	0.8	5.5	AA 1050
29	1300	0.8	4	AA 2024
30	2000	0.5	6.5	AA 2024

2.4 Sparse proper generalized decomposition technique

The sparse Proper Generalized Decomposition (sPGD) technique aims to capture an objective function by means of the separation of variables as shown in eq. 1.

$$\boldsymbol{f}(p_{1,}p_{2,\dots,}p_n) \approx \mathbf{a}(p_{1,}p_{2,\dots,}p_n) = \sum_{m=1}^{M} \boldsymbol{u}^m g_1^m(p_1) g_2^m(p_2) \dots g_n^m(p_n) \tag{1}$$

where M is the number of enrichments (a.k.a. low-rank approximations) in the approximation and n is the number of dimensions in the parametric space.

Let's assume that the output function is known at several points inside the parametric space as shown in eq. 2.

$$f(p^s) = f_s; \quad s = 1, \dots, S \tag{2}$$

The sPGD solution is obtained by minimizing the following functional:

$$\sum_{s=1}^{S} a_s(a_s - f_s) = 0 \tag{3}$$

More in detail, a greedy procedure, where the previous knowns are fixed when looking at the new enrichment, plus an altered direction scheme are in charge of controlling the approximation.

3 RESULTS AND DISCUSSION

This section presents the influences of some identified process parameters and the process answers at their variation achieved by the methodology outlined in Sec.2. Specifically, the joint efficiency was evaluated by measuring the maximum temperature of the polycarbonate plate in a specific contact area with the friction-heated aluminum side, and the volume interlocking between these two materials. The choice of these outputs is related to thermal deterioration problems, which the polymers are subject at elevated temperatures, and to the strength of the connection, which is strictly connected to the reached interaction between the two plates.

3.1 FEM results

In Fig. 4, there are images showing the typical temperature distribution, as a result of the 2D proposed FE model, at the end of phase “a” and phase “b” highlighted in Fig. 3.

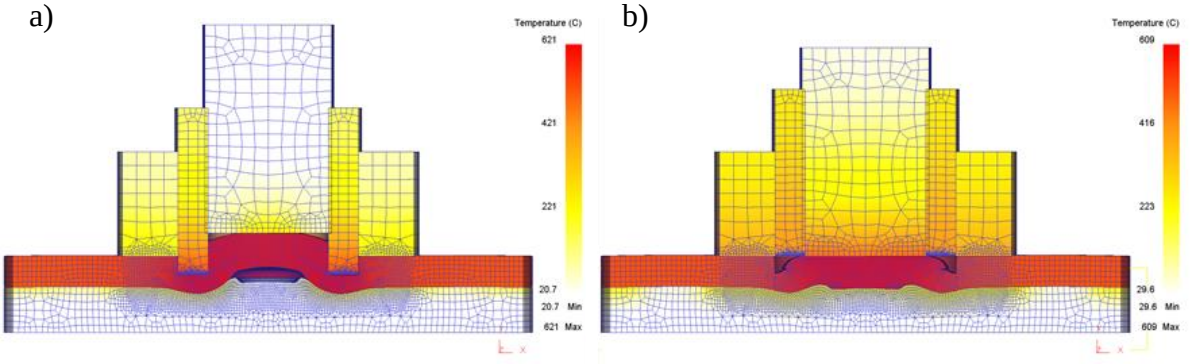

Figure 4: Typical result for the FSjP process simulation, at the end of the phase “a” (a) and “b” (b)

The maximum temperature is located on the Aluminum plate in the area strictly connected to the rotating rigid tool. Herein, the metal is strongly stirred up to reach the melting temperature. The fluid material is first gathered below the pin (Fig. 4a) and, subsequently, pushed to the plastic plate resulting in a mechanical interlocking between the surfaces of the two parts (Fig. 4b). The joint performance is further consolidated by micromechanical adhesion, which is also function of the reached temperatures coupled to the generated contact pressures.

According to what above said, the selected outputs were: the maximum temperature of the peak and of the valley, which refer both to the polycarbonate sheet, and the interlocking area calculated as highlighted in Fig.5.

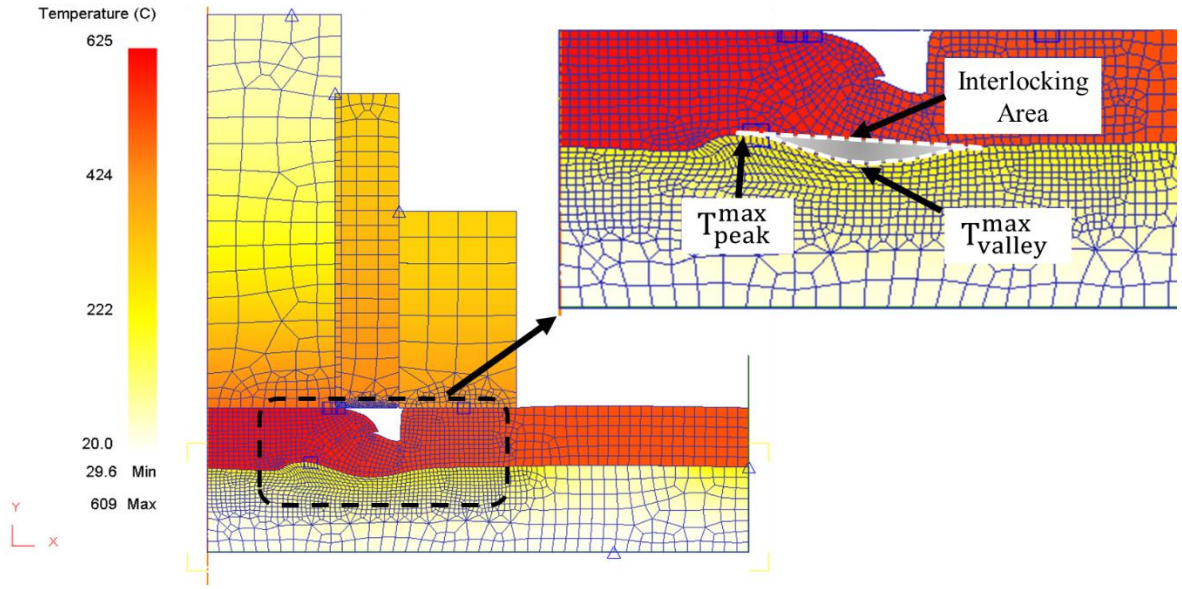

Figure 5: The selected results: the maximum temperature of the peak, the maximum temperature of the valley and the interlocking area

For the joining conditions reported in Table 4, the obtained minimum and maximum values extracted by the conducted FE simulation are reported in Table 5 for the different tests.

Table 5: Range of the results obtained by the FE simulations

Factors	Symbol	Unit	Min	Max
maximum temperature of the peak	T^{max}_{peak}	°C	169	335
maximum temperature of the valley	T^{max}_{valley}	°C	146	304
Interlocking	$A_{interlock}$	mm^2	25.44	4.59

3.2 Sensitivity analysis of the investigated process parameters

The performed sensitivity analysis showed the individual influence of the selected joining parameters. The possible interactions among the highlighted variables were not taken into account. Fig. 6, 7 and 8 show respectively the influence of RS, JT and PD on T^{max}_{valley} and $A_{interlock}$.

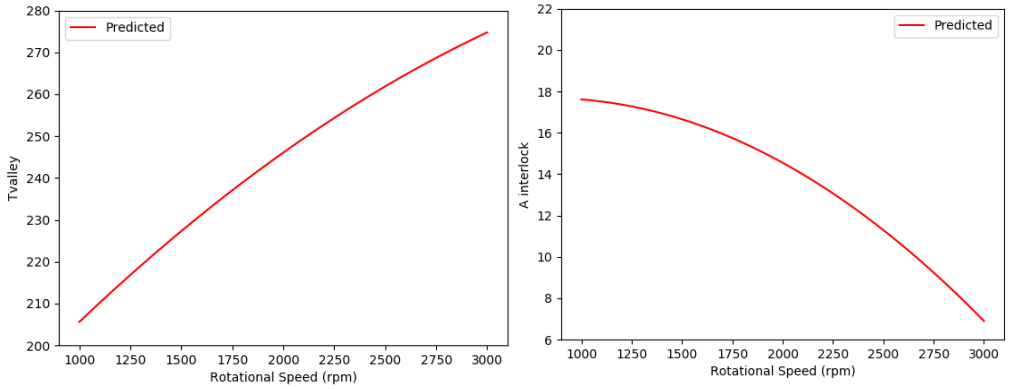

Figure 6: Influence of RS. Left, T_{valley}^{max} for different RS. Right, $V_{interlock}$ for different RS

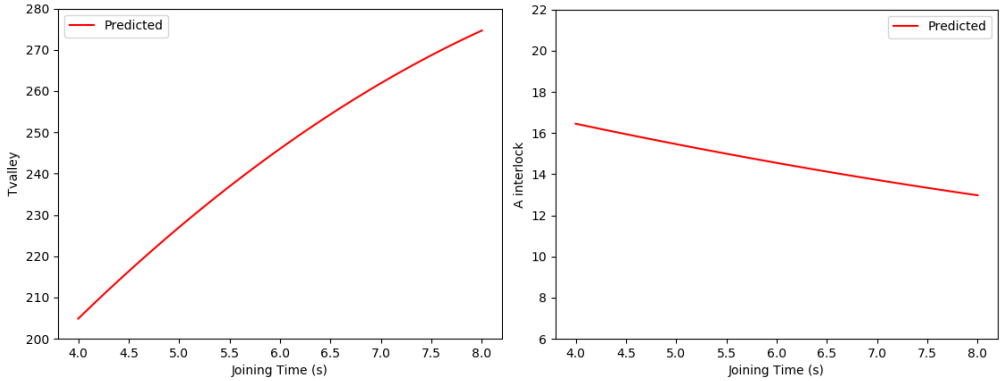

Figure 7: Influence of JT. Left, T_{valley}^{max} for different JT. Right, $V_{interlock}$ for different JT

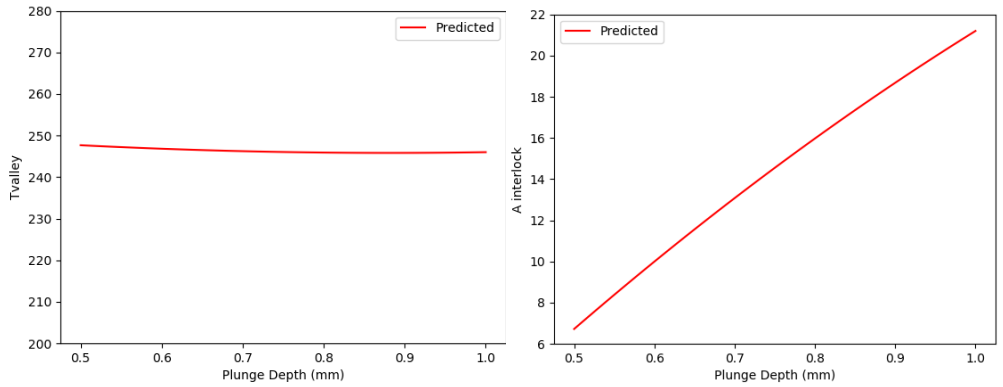

Figure 8: Influence of PD. Left, T_{valley}^{max} for different PD. Right, $V_{interlock}$ for different PD

Before discussing the above reported figures, it deserves to be highlighted that:

1) the graphs of $\boldsymbol{T_{peak}^{max}}$ were not reported because resulted similar to $\boldsymbol{T_{valley}^{max}}$.

2) the interlocking and the $\boldsymbol{T_{valley}^{max}}$ are, respectively, greater than about 50% and smaller than about 15% with the AA 1050 respect to the AA 2024.

3) the current model is just a regression that matches the points that are established. Therefore, from these data it is possible to extract some important consideration.

Going deeply to the result analysis, first, from Fig. 6 and 7, it can be noted that there is a growth of $\boldsymbol{T_{valley}^{max}}$ as RS and JT rise because of an increment of the generated friction heating, while, at the same time, there is a decrement in volume interlocking owing to a softening of the joined area during the pushing phase of the pin. The growth in volume interlocking vs JT after a minimum point can be, instead, ascribed to the melting of the polycarbonate as a result of the heat transmitted from the aluminum. Anyway, this evidence needs additional tests to be validated considering also the interdependency among the process variables. Finally, Fig. 8 illustrates an evident effect of PD in volume interlocking while this can be almost neglected for the trend of $\boldsymbol{T_{valley}^{max}}$. This results was justified because of the quantity of material moved that is strictly related the sleeve plunging inside the aluminum while the effect on the generated heat is less significant owing to the reduced increment of the contact surface in respect of the total contact area of the rigid tool.

3.3 sPGD results

For this particular problem the three scalar quantities of interest were taken into account, i.e., T_{peak}^{max}, T_{valley}^{max} and $A_{interlock}$. All these three quantities depend on the four analyzed process parameters and, therefore, the problem was reformulated as finding:

$$T_{peak}^{max} = f_1(RS; PD; JT; AA)$$
$$T_{valley}^{max} = f_2(RS; PD; JT; AA)$$
$$A_{interlock} = f_3(RS; PD; JT; AA)$$

The dataset used all the 30 points generated by means of a hypercube latin. From these 30 points, 24 points are kept in the training set whereas the other 6 are left outside to validate the results. The interpolation functions used in the parametric space are Chebyshev polynomials up to linear interpolation, more polynomial order was tested but the results did not present better results. Fig. 9 shows the analysis involving T_{peak}^{max}.

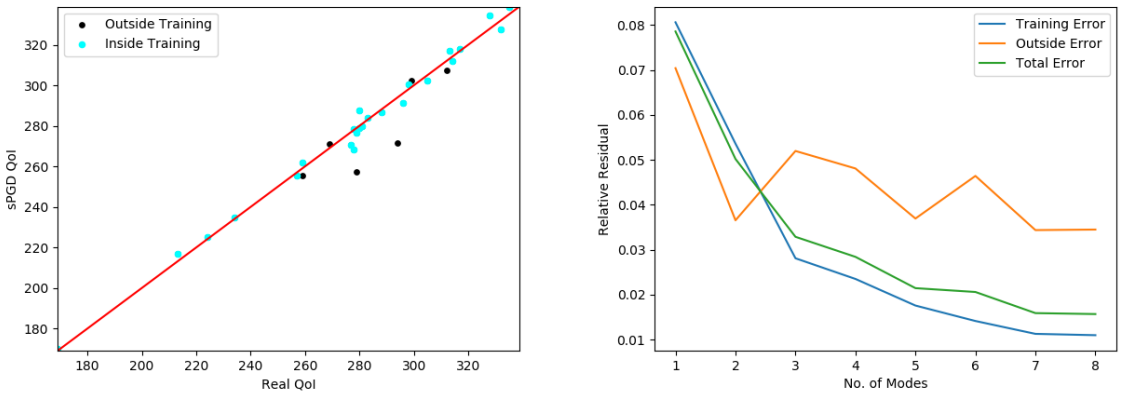

Figure 9: T_{peak}^{max}. Left, real versus predicted. Right, convergence for different number of modes

On the left side, it can be seen the real versus the predicted quantity of interest. There are two different colors, blue and black points, related to the training and outside training datasets, respectively. On the right-hand side, the relative residual of equation 3 is shown as the number of enrichments are increased (blue line). The residual can also be evaluated at the 6 points outside the training, generating the orange line. The results present a 1-2% relative error in the training, whereas 3-4% outside the training.

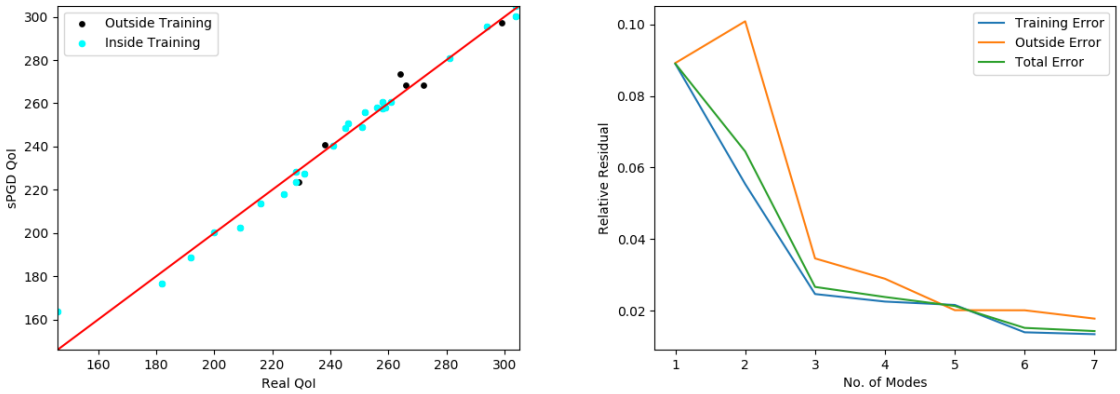

Figure 10: T_{valley}^{max}.. Left, real versus predicted. Right, convergence for different number of modes

Fig. 10 shows the same results as Fig. 9, but applied to T_{valley}^{max}. In this particular case, the regression result was better than in the previous case, achieving relative errors of 2% in both training and outside training. Finally, Fig. 11 shows the regression results for the $A_{interlock}$ variable. As it can be observed, the regression results are quite acceptable as well.

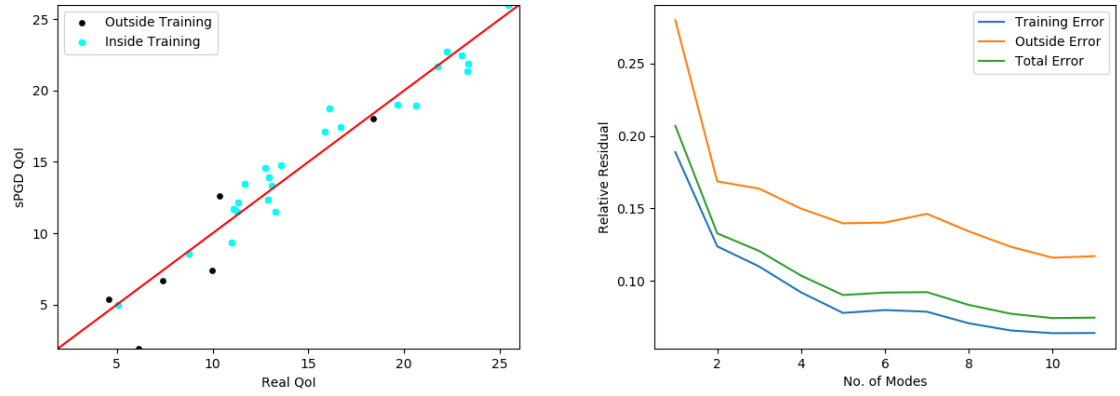

Figure 11: $A_{interlock}$. Left, real versus predicted. Right, convergence for different number of modes

4 CONCLUSIONS

The Friction Spot Joining was investigated in joining dissimilar materials, i.e., lightweight alloys and plastics. Specifically, a 2D axisymmetric finite element model was set in order to be

able to predict the performance of the obtained connections. Several simulation were ran changing the main process parameters according to a DoE planning. The monitored outputs were chosen taking into account the degradation problems that can occur on the surface of the joined plastic and the achieved mechanical interlocking, which affects the joint strength. Specifically, a sensitivity analysis allowed to understand the influence of each of the investigated process parameters on the highlighted outputs while the use of the sPGD technique allowed to define interpolation functions able to predict the quantities of interest, properly. The influences of the tool rotational speed, plunge depth, joining time and material properties of the process were evaluated, preliminary. Additional numerical tests, confirmed by experimental evidences, are required to validate what observed looking also at the relationship among the explored variables.

REFERENCES

[1] Goushegir, S.M., dos Santos J.F. and Amancio-Filho S.T. Friction Spot Joining of aluminum AA2024/carbon-fiber reinforced poly(phenylene sulfide) composite single lap joints: Microstructure and mechanical performance. *Mater. Des.* (2014) **54**:196–206.

[2] Blaga, L., Dos Santos J.F., Bancila, R. and Amancio-Filho, S.T. Friction Riveting (FricRiveting) as a new joining technique in GFRP lightweight bridge construction. *Constr. Build. Mater.* (2015) **80** 167–79.

[3] Amancio-Filho, S.T. and dos Santos, J.F. EP2329905B1 Method for joining metal and plastic workpieces. European Patent (2012)

[4] Schilling, C. and Dos Santos, J. Method and Device for Linking at Least Two Adjoining Work Pieces by Friction Welding (2001)

[5] Goushegir, S.M., dos Santos J.F. and Amancio-Filho S.T. Influence of process parameters on mechanical performance and bonding area of AA2024/carbon-fiber-reinforced poly(phenylene sulfide) friction spot single lap joints. *Mater. Des.* (2015) **83** 431–42.

[6] Adibeig, M.R., Marami, G., Saeimi-Sadigh, M.A. and da Silva, L.F.M. Experimental and numerical study of polyethylene hybrid joints: Friction stir spot welded joints reinforced with adhesive. *Int. J. Adhes. Adhes.* (2020) **98** 102555.

[7] Yu, M., Li, W.Y., Li, J.L. and Chao, Y.J. Modelling of entire friction stir welding process by explicit finite element method. *Mater. Sci. Tech.* (2012) **28** 812–817.

[8] Malik, V., Sanjeev, N.K., Hebbar, H.S. and Kailas, S.V. Investigations on the effect of various tool pin profiles in friction stir welding using finite element simulations. *Proc. Eng.* (2014) **97** 1060–8.

[9] Ansari, M.A., Samanta, A., Behnagh, R.A. and Ding H An efficient coupled Eulerian-Lagrangian finite element model for friction stir processing. *Int. J. Adv. Manuf. Technol.* (2019) **101** 1495–508

[10] Chen, K., Liu, X. and Ni, J. A review of friction stir–based processes for joining dissimilar materials *Int. J. Adv. Manuf. Technol.* (2019) **104** 1709–1731.

[11] Chiumenti, M., Cervera, M., Agelet de Saracibar, C. and Dialami, N. Numerical modeling of friction stir welding processes *Comput. Methods Appl. Mech. Eng.* (2013) **254** 353–369.

[12] Buffa, G., Hua, J., Shivpuri, R. and Fratini, L. A continuum based fem model for friction stir welding - Model development *Mater. Sci. Eng. A (*2006*)* **419** 389–396.

[13] Fuller, J.J. and Marotta, E.E. Thermal Contact Conductance of Metal/Polymer Joints: An Analytical and Experimental Investigation. *J. Thermophys. Heat Transf.* (2001) **15** 228–38.

[14] Johnson, G.R. and Cook, W.H. A constitutive model and data from metals subjected to large strains, high strain rates and high temperatures *Proc. 7th {I}nt. {S}ymp. on {B}allistics, {T}he {H}ague, {N}etherlands (*1983*).*

[15] Eide, H.O.S. and Melby, E.A. Blast loaded aluminium plates Experiments and numerical

simulations. *Master Thesis* (2013) 1–139.
[16] Asad, M., Girardin, F., Mabrouki, T. and Rigal, J.F. Dry cutting study of an aluminium alloy (A2024-T351): A numerical and experimental approach. *Int. J. Mater. Form.* (2008) **48** 1187-1197.
[17] Duan, Y., Saigal, A., Greif, R. and Zimmerman, M.A. A uniform phenomenological constitutive model for glassy and semicrystalline polymers *Polym. Eng. Sci.* (2001) **41** 1322–1328.